A&A 465, 613–619 (2007)
DOI: 10.1051/0004-6361:20066573

Astronomy & Astrophysics

Turbulent propagation of high-energy electrons in a solar coronal loop

A. V. Stepanov[1], T. Yokoyama[2], K. Shibasaki[3], and V. F. Melnikov[4]

[1] Pulkovo Observatory, Russian Academy of Sciences, 65 Pulkovo, 196140 St. Petersburg, Russia
e-mail: stepanov@gao.spb.ru
[2] Department of Earth and Planetary Science, University of Tokyo, 113-0033, Japan
[3] National Astronomical Observatory, Nobeyama, Minamimaki, Minamisaku, 384-1305 Nagano, Japan
[4] Radiophysical Research Institute, 25 B. Pecherskaya, 603600 Nizhny Novgorod, Russia

Received 16 October 2006 / Accepted 13 December 2006

ABSTRACT

Aims. We study the solar flare on 28 August 1999 observed by the Nobeyama Radioheliograph at 17 and 34 GHz and analyze the unusual behavior of microwave source (a coronal loop) after injections of high-energy electrons. The observations reveal a propagation velocity of the emission front along the loop of about 10^4 km s^{-1}, which is 30 times less than the velocity of high-energy electrons generating gyrosynchrotron emission at 17 and 34 GHz. The main goal is to understand the physical origin of this electron propagation.
Methods. We interpret this anomalous propagation in terms of the collective effects of relativistic electrons interacting with plasma turbulence. A cloud of highly energetic electrons responsible for microwave emission generates low-frequency whistler waves, and a turbulent "wall" in the loop is formed.
Results. The electrons undergo strong resonant scattering due to wave-particle interaction, and the emission front propagates with the wave phase velocity, which is much lower than the particle velocity.

Key words. Sun: flares – Sun: corona – Sun: radio radiation

1. Introduction

The mechanisms of charged particle acceleration, propagation, and emission during solar flares are still open questions. Recent radio observations with large radiotelescopes (VLA, RATAN–600, NoRH, SSRT) and space observations in the UV and X-ray bands (TRACE, Yohkoh, RHESSI) supply key information about the energy-release processes on the Sun. Observations have shown that a flare site usually consists of a number of magnetic loops. These loops are actually the magnetic traps for energetic particles. In some cases, a flare appears as a single or double loop structure (Sakai & de Jager 1996).

The signatures of accelerated electrons are mainly observed in hard X-rays and radio bands. There is an ongoing discussion in the literature concerning the dynamics and propagation of high-energy electrons in coronal magnetic loops (see e.g. Wentzel 1976; Melrose & Brown 1976; Bespalov et al. 1987; Hulot et al. 1989; Lee & Gary 1994; Alexander 1990; MacKinnon 1991; Fletcher 1997; Melnikov & Magun 1998; Lee et al. 2000; Stepanov & Tsap 2002; Melnikov et al. 2002; Aschwanden 2002). Two extreme approaches are usually used in this context: (i) free propagation ("time-of-flight" approach), which suggests that there are no particle-particle or wave-particle collisions; (ii) collision-dominated propagation. The collision rate can be so high that a strong pitch angle diffusion is realized.

Strong diffusion means that the mean time of pitch-angle scattering by about $\pi/2$ is less than the free travel time of particles in a loop, $t_d < t_0 = L/V$. Here L is the loop length and V the particle velocity. This was the basis of an idea by Budker et al. (1971) concerning the trapping of hot collisional plasma: instead of plasma free-propagation along the magnetic-trap axis, slow diffuse extension is obtained. Under a typical solar flare loop condition the ≥100 keV electrons are collisionless on a time scale of a few seconds (Stepanov & Tsap 2002). In order to describe the strong diffusion of accelerated electrons in a flare loop, the wave-particle interaction should therefore be taken into account. A particle interacting with small-scale waves stochastically changes its velocity direction; i.e. the particle motion along the loop axis can be described as diffusion. An anomalous viscosity appears to result from wave turbulence and to slow down the particle motion. As a result the particle propagation velocity is close to the wave phase velocity (phase-type resonance). This "turbulent propagation" regime, which is possible for quite powerful sources of energetic particles, is described in terms of the quasi-linear diffusion of particles on waves (Trakhtengerts 1984). The dynamics of the expansion of slightly anisotropic energetic electron flux in turbulent space plasma was analyzed by Bespalov & Efremova (1993) for the case of dense plasma, $\omega_p^2 \gg \Omega^2$. Here ω_p is the electron plasma frequency, and Ω the electron gyrofrequency. In this case an energetic electron cloud generates plasma (Langmuir) waves with relatively low phase velocity and forms a "turbulent wall" on its front (self-consistent expansion). Another case of turbulent propagation is also possible when the particle flux propagates through the plasma with a constant level of plasma turbulence (Bespalov & Efremova 1993).

It should be noted that the "turbulent propagation" regime was investigated earlier for the expansion of hot thermal plasma in a flare loop (Brown et al. 1987; Smith & Lillienquist 1979; Batchelor et al. 1985). It was demonstrated that the expansion

velocity is close to ion-sound velocity and driven by ion-sound turbulence at the plasma-cloud front.

The consequences of strong diffusion of energetic electrons propagating at whistler velocity, and ions propagating at Alfven velocity in solar flares were considered by Bespalov et al. (1987). Using a turbulent propagation approach, they built a one-step acceleration model to explain the time lags in gamma-ray emission peaks vs. hard X-ray peaks, as well as some peculiarities in solar hard X-ray spectra and particle fluxes in interplanetary space.

The interpretations by Bespalov et al. (1987) were, in fact, indirect indications of possible turbulent propagation events. There are a few examples of radio observations that have succeeded in detecting the motion of accelerated electrons as a series of images. Bastian et al. (1994) reported the motion at 3×10^3 km s^{-1} using VLA observations at 8.4 and 15 GHz. White et al. (2000) found the propagation of a nonthermal disturbance at a velocity of 2.6×10^4 km s^{-1} at 330 MHz. Yokoyama et al. (2002) report on their observation of a very intriguing nonthermal event on 28 August 1999. Using the NoRH imaging data at 17 GHz, they found two types of moving microwave sources inside a flaring loop classified by speed. The radio emission was explained in terms of gyrosynchrotron emission from high-energy electrons in a coronal loop with the magnetic field $B \approx$ 150–200 G. One moving source propagated at a speed of about 10^5 km s^{-1}, and the other at a speed of $\leq 10^4$ km s^{-1}. The case of $\approx 10^5$ km s^{-1} was interpreted by Yokoyama et al. (2002) as the first imaging observation of streaming relativistic electrons, which have large (>70°) pitch angles after injection into a flare loop (see also Hanaoka 1999). The case of slower propagation, $v \leq 10^4$ km s^{-1}, is very challenging and puzzling. It is known (e.g. Bastian 1999), that the main contribution to ≥17 GHz gyrosynchrotron emission in the magnetic field of $B \approx$ 150–200 G is provided mainly with ∼(0.5–3) MeV electrons, so the question arises as to why relativistic electrons propagate so slowly in a coronal loop.

This paper is an attempt to interpret the anomalously slow propagation ($\approx 10^4$ km s^{-1}) of the microwave source in the flare of 1999 August 28 in terms of strong pitch-angle diffusion, which forms a "turbulent wall" and reduces the apparent propagation speed of relativistic electrons.

2. Observations

The flare event of 1999 August 28, 00:53–01:00 UT was observed with GOES, SOHO/MDI, BATSE, and with the Nobeyama Radioheliograph (NoRH) at 17 and 34 GHz (Fig. 1). The flare occurred in the active region NOAA 8674 at S25 W11 and had an optical importance of 1F. The GOES soft X-ray class was M2.8. A detailed description of this flare was given by Yokoyama et al. (2002).

The microwave structure of the event consists of two main sources (Fig. 2, upper left panel). It follows from the spatial co-alignment with SOHO/MDI magnetograms that the compact source with magnetic field value $B \sim 650$ G is located near a sunspot. This point source (<10 arcsec) was unresolved by NoRH. The well-resolved, elongated loop-like source with extension ≈65 arcsec (apparent length $L_{\rm app} \approx 4.5 \times 10^9$ cm) was situated close to the compact source. It is seen especially well at frequency 34 GHz (Fig. 2, upper right panel). Using the potential magnetic field approximation obtained by extending the magnetogram data to the photosphere by SOHO/MDI (Fig. 2, lower left panel), we concluded that the magnetic field values along the loop vary from 255 G (maximum) to 120 G (minimum). It

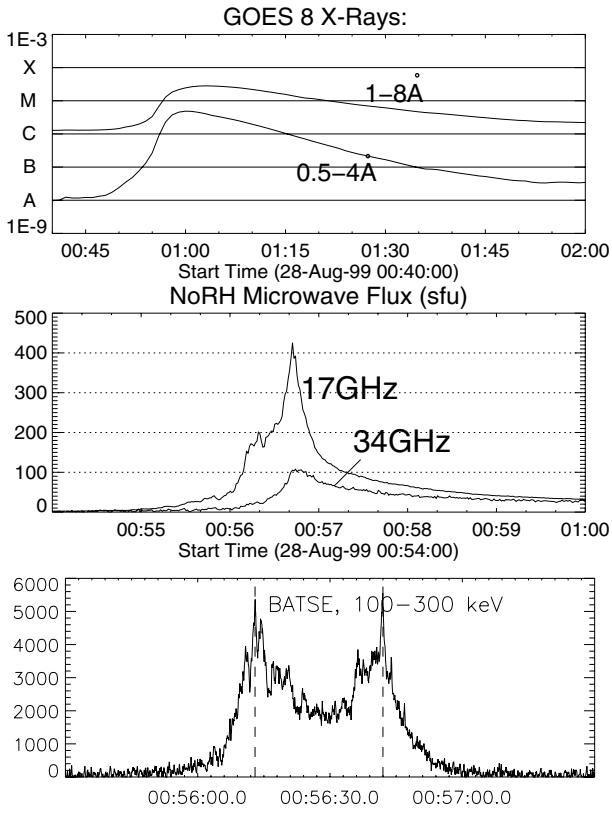

Fig. 1. The time profiles of the 1999 August 28 flare. *Top panel*: soft X-ray light curves in the band of 0.5–4 Å and of 1–8 Å obtained by the GOES satellite. *Middle panel*: microwave flux in sfu at 17 and 34 GHz obtained with NoRH. *Bottom panel*: hard X-ray flux at energy interval 100–300 keV, the vertical dashed lines show the positions of two main peaks at 00:56:13 and 00:56:42 UT.

means that the mirror ratio of extended coronal loop is quite low, $\sigma = B_{\rm max}/B_{\rm min} \approx 2$. Yokoyama et al. (2002) concluded that radio emission from the elongated source is due to a nonthermal gyrosynchrotron mechanism. The peak of brightness temperature at 17 GHz was estimated as $T_{\rm b} \approx 10^7$ K at 00:56:42 UT.

We suppose that the plasma temperature in the extended loop before the first electron injection (00:56:10 UT) is near the coronal temperature ($T \approx 2 \times 10^6$ K). For the estimation of plasma density in the extended source, we may use the radio data. Indeed, there is no NoRH detection of the optically thin bremsstrahlung emission at 17 and 34 GHz from the loop source before the flare. Taking into account that the bremsstrahlung radio emission flux is proportional to $n^2 T^{-1/2}$ and that plasma temperature $T \approx 2 \times 10^6$ K, we can conclude that the number density of the loop plasma before the flare was below or equal the NoRH detection limit, $n \approx 7 \times 10^9$ cm^{-3}. Corresponding electron plasma frequency $\omega_{\rm p} \approx 5 \times 10^9$ s^{-1}, and the electron cyclotron frequency for mean magnetic field of the loop $B = 150$ G is about $\Omega \approx 2.6 \times 10^9$ s^{-1} $\approx 0.5\omega_{\rm p}$. Hence the plasma beta parameter in a large loop before the flare was quite low, $\beta = 8\pi n \kappa T / B^2 \approx 2.2 \times 10^{-3}$.

The NoRH maps and time profiles of the burst at 17 and 34 GHz as well as BATSE hard X-ray data suggest that there were several injections of super-thermal electrons into the large coronal loop. From Fig. 3 we see that at the initial stage of the flare (00:56:00–00:56:21 UT) there are at least two signatures of injection and propagation of high-energetic electrons in the large loop during the radio burst. The propagation event after the first

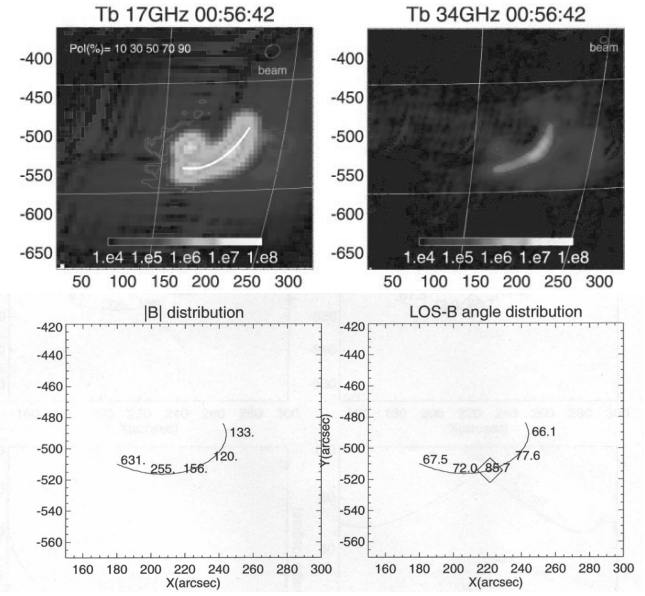

Fig. 2. Nobeyama 17 and 34 GHz image of the flare on 28 August 1999 at the peak time (*top*). The white line at 17 GHz image indicates the propagation trajectory of a microwave source. The bottom left-hand corner of the loop corresponds to 0 km on the vertical axis of Fig. 3. Distributions of the magnetic field (*bottom left*) and viewing angle (*bottom right*) have shown as inferred from the SOHO/MDI magnetograms.

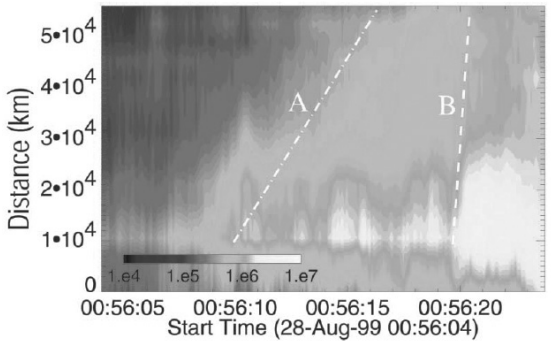

Fig. 3. Time variation of the 17 GHz intensity distribution along the microwave loop indicated by the solid white line in the top left panel of Fig. 2. The dash-dotted line "A" and dashed line "B" correspond to the speeds $\approx 10^4$ km s^{-1} and $\approx 10^5$ km s^{-1} (Yokoyama et al. 2002).

injection ("A") starts at 00:56:10 UT and has an apparent velocity $\approx 7 \times 10^3$ km s^{-1}. If we assume that the loop is a semicircle, the length of the traveling path is about $\pi/2$ times greater; hence, the propagation velocity of the emission front in the case "A" can be about $V_a \approx 10^4$ km s^{-1}. The second event ("B") was faster and the propagation velocity was estimated as $V_b \approx 10^5$ km s^{-1}. The emission front in the event "B" can be interpreted as an injection of ~1 MeV electrons with pitch-angle $\theta = \arccos(V_b/c) \approx 70°$ (see e.g. Yokoyama et al. 2002).

To construct the model of strong turbulent diffusion (Trakhtengerts 1984), we also need to know the power flux of particle source $I \approx n_1 V_a$, which is the number density of high-energy electrons n_1. Although the main contribution to ≥17 GHz emission in the magnetic field $B \sim$ 150–200 G is mainly provided by ~1 MeV electrons (Bastian 1999), the particles with lower energies also take part in gyrosynchrotron emission at these frequencies. Our evaluations have shown that, for this purpose, one can choose the low-energy limit for resonance

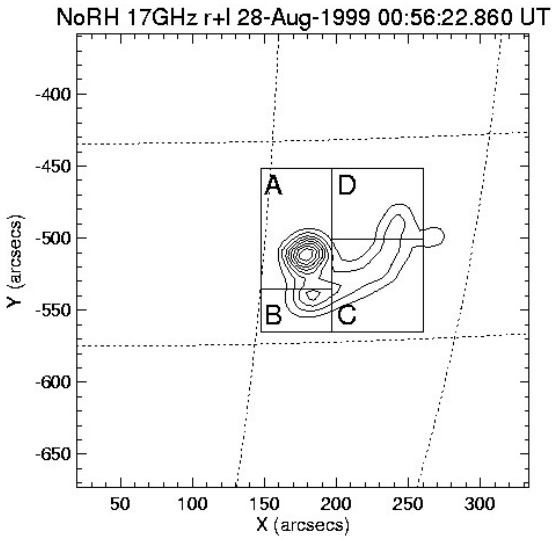

Fig. 4. 2D picture of the flare at 17 GHz (00:56:23 UT) divided in four boxes.

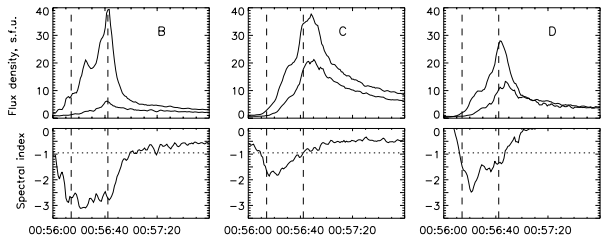

Fig. 5. *Top panel*: NoRH time profiles of the flux densities from the 20″ × 20″ boxes located at the loop top (the center of region C in Fig. 4) and the footpoints (region B and region D in Fig. 4) of the 1999 August 28 flare. *Bottom panel*: the corresponding time profiles of the microwave spectral index between 17 and 34 GHz. Vertical dashed lines indicate the moments of the two hard X-ray emission peaks, at 00:56:13 and 00:56:42 UT.

electrons $E_0 = 500$ keV. From NoRH observations at 17 GHz and 34 GHz we can estimate the density of radio-emitting electrons. Actually, we do not know the real distribution function of high-energy electrons. For the sake of illustration and, in particular, to estimate the minimal value of the density of high-energy electrons we nevertheless suppose that accelerated electrons have a power-law energy spectrum of $\propto E^{-\delta}$.

We divided the observed source into 4 regions (see Fig. 4). Region "A" includes the very compact source, possibly an unresolved compact loop located near a sunspot with the magnetic field $B \approx 650$ G in the spot vicinity. Regions "B", "C", and "D" cover the extended flaring loop, which is the most important one for our the current study. The footpoints of the loop are located in regions "B" and "D" and the looptop in region "C".

In the upper panel of Fig. 5 we show NoRH time profiles of the flux densities from the 20″ × 20″ boxes located at the loop top (the center of region C in Fig. 5) and the footpoints (regions B and D in Fig. 4). In the bottom panel are the corresponding time profiles of the microwave spectral index between 17 and 34 GHz.

Figure 5 shows that in the time interval of the first injections (00:56:10–00:56:16,5 UT) where unusual propagating sources appear, the frequency spectral index is in the range $-2.5 \div -3.0$ in region "B". This corresponds to the value of the power-law electron energy spectral index $\delta \approx$ 4.5–5.0 if

one considers the exact formalism for gyrosynchrotron emission (Ramaty 1969; Fleishman & Melnikov 2003). In regions "C" and "D" frequency spectral index is lower, possibly due to the smaller magnetic field there (Melnikov 2006). To evaluate the energetic electron number density near the propagation start (region "B") let us take the electron power-law index $\delta = 5.0$, the source depth = 10^9 cm, magnetic field $B = 150$ G, and view angle = 80 degrees. Using the formalism of Ramaty (1969), we obtain $n_1(>0.5\ \mathrm{MeV}) \approx 3 \times 10^3\ \mathrm{cm}^{-3}$. Note that the approximation formulas of Dulk (1985) give almost the same result, so that a flux power of the injection can be estimated as $I = n_1 V_\mathrm{a} \approx 3 \times 10^{12}\ \mathrm{cm}^{-2}\ \mathrm{s}^{-1}$.

3. The model

The event under consideration consists of two flaring loops (Figs. 2–4). The first unresolved compact loop is located near a sunspot with the magnetic field in the spot vicinity $B \approx 650$ G. We suppose that this faint loop is an injector of both high-energy electrons and dense thermal plasma into the large coronal loop. This kind of particle intrusion can be due to loop–loop coalescence (see e.g. Hanaoka 1999), in particular, to the ballooning instability (Shibasaki 2001) or to magnetic reconnection (Yokoyama & Shibata 1995). Accelerated particles can penetrate the large loop and provoke the radio emission, at 17 and 34 GHz, and hard X-ray emission. During the first injection of high-energy electrons the front of radio emission propagated along the loop with unusually low velocity, $\approx 10^4$ km s^{-1}, which is 30 times lower than the velocity of relativistic electrons.

We have to find the physical reason for this unusually slow speed of 17 GHz emission front. At first glance, this value is about the velocity of thermal plasma with the temperature $T \approx 10^7$ K. But the gyrosynchrotron emission of such thermal plasma is much weaker at 17 GHz. The value of the Alfven velocity $V_\mathrm{A} = B(4\pi nM)^{-1/2}$ fits well to 10^4 km s^{-1}, if plasma density $n \approx 10^{10}\ \mathrm{cm}^{-3}$ and the magnetic field value $B \approx 500$ G. This value for the magnetic field is too high for the elongated source (Fig. 2). Moreover, there are no evident physical reasons for the expansion of 17 GHz radiated electrons with the Alfven velocity.

We suppose that this slow propagation of a cloud of high-energy electrons is due to the scattering of electrons on small-scale turbulence. A particle interacting with waves stochastically changes its velocity direction; i.e. a turbulent "wall" is formed and a particle propagation velocity approaches the wave phase velocity. This "turbulent propagation" regime is possible for quite a powerful source of energetic particles, $I^* \approx cB\sigma/4\pi eL$ (Trakhtengerts 1984). Our case ($B \approx 150$ G, $L \approx (\pi/2)L_\mathrm{app} \approx 7 \times 10^9$ cm, $\sigma \approx 2$) gives $I^* \approx 2 \times 10^{11}\ \mathrm{cm}^{-2}\ \mathrm{s}^{-1}$. This value is more than one order of magnitude lower than the flux power of the injection source, $I \approx 3 \times 10^{12}\ \mathrm{cm}^{-2}\ \mathrm{s}^{-1}$, estimated in Sect. 2.

The most effective scattering of super-thermal electrons under solar corona conditions ($\omega_\mathrm{p} > \Omega$) is due to the resonant interaction of electrons and whistlers (Wentzel 1976; Melrose & Brown 1976; Bespalov et al. 1987, 1991). The source power for our loop parameters is large enough, $I \sim 10I^*$, and strong diffusion regime can realize. We suggest that in the event of 1999 August 28, the electrons injected at 00:56:10 UT into the coronal loop generated whistler turbulence and scattered on the whistlers. As the result the bulk of energetic electrons propagates with the velocity close to the whistler phase velocity, which is much lower than the velocity of relativistic electrons.

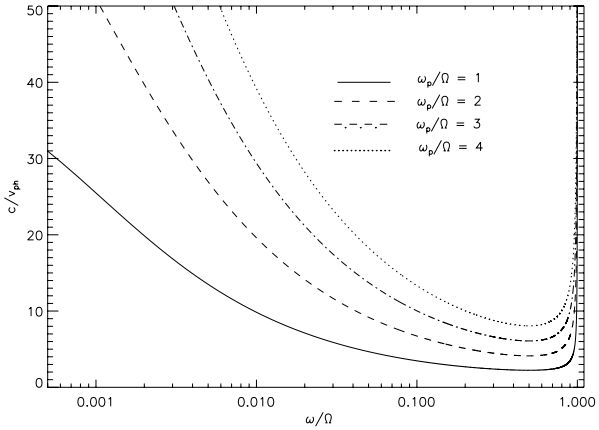

Fig. 6. Inversed phase velocity of whistler waves vs. $x = \omega/\Omega$ for $y = \omega_\mathrm{p}/\Omega = 1, 2, 3, 4$.

4. Turbulent propagation of energetic electrons in a coronal loop

Another possible reason for an anomalously slow propagation of high-energy electrons is the generation of Langmuir waves by the electrons themselves. In this case, the velocity of the bulk of energetic electrons is close to the electron thermal velocity of background plasma (Bespalov & Efremova 1993). In this section we consider both possibilities.

4.1. "Wall" due to whistler turbulence

It is well known that the most important small-scale turbulence that determines the behavior of high-energy electrons in solar coronal loops is whistler-wave turbulence (Wentzel 1976; Melrose & Brown 1976; Bespalov et al. 1987, 1991; Stepanov & Tsap 2002). The anisotropy threshold for whistler instability is quite low. For example, cold background plasma and energetic electrons with temperature anisotropy, $T_\perp \neq T_\parallel$, are stable against Langmuir wave excitation, but unstable against whistlers.

The whistler phase velocity ω/k for wave propagation along the magnetic field in the cold plasma approximation is determined from the dispersion relation (Brambilla 1998)

$$N^2 = \left(\frac{kc}{\omega}\right)^2 = 1 - \frac{y^2}{x(x-1)} - \frac{\mu y^2}{x(x+\mu)} \qquad (1)$$

where $y = \omega_\mathrm{p}/\Omega$, $x = \omega/\Omega$, ω_p is the electron plasma frequency, Ω and $\Omega_i = \mu\Omega$ are the electron and ion gyrofrequencies, and $\mu = m/M = 1/1836$. The whistler frequency is ω ($\Omega_i \ll \omega \ll \Omega$). Figure 6 shows the inverse whistler phase velocity vs. x for different y. It has a minimum $N = kc/\omega \approx (2.3\text{–}8.8)$ near $x = \omega/\Omega \approx 0.5$ and grows for $x \to 1$ and for $x \to \mu$. In our case the emission fronts after the first injection move with a velocity of about $3 \times 10^{-2}c$. We will find the conditions under which the whistler phase velocity $\omega/k \approx 3 \times 10^{-2}c$.

As follows from the plot of phase velocity vs. x (Fig. 6), two cases should be possible:

1. high-frequency whistlers ($\omega \to \Omega$), and
2. low-frequency whistlers ($\omega \to \Omega_i$).

We have to determine first which case fits the observed velocity of propagation of the radio source at about 10^4 km s^{-1}.

In accordance with our model, the whistlers can be generated by a group of energetic electrons anisotropically injected into a large magnetic loop from a compact loop due to loop–loop interaction. Evidence of the transverse anisotropy of high-energy electrons in extended flaring loops was obtained from NoRH observations of radio-brightness spatial profiles along the loops (Melnikov et al. 2002). It is not excluded that the injection at 00:56:10 UT (event "A" in Fig. 4) was oblique to the magnetic field. Such electrons have an anisotropic distribution, which can be represented as

$$F \propto n_1 E^{-\delta} \varphi(\theta). \tag{2}$$

Here $E = mc^2(\gamma - 1)$ is the electron energy, γ the Lorenz factor, and $\varphi(\theta)$ describes the pitch-angle anisotropy. For example, the loss-cone anisotropy suggests $\varphi(\theta) = H(\theta)$, where $H(\theta)$ is the Heaviside step function: $H(\theta) = 1$ for $\theta^* < \theta < \pi/2$, $H(\theta) = 0$ for $0 < \theta < \theta^*$. Due to the inverse population of fast particles in the direction perpendicular to the magnetic field the electrons interact with whistlers most effectively under the cyclotron resonance condition (normal Doppler effect):

$$\omega - k_\parallel V_\parallel - \Omega/\gamma = 0. \tag{3}$$

The whistler growth rate for the electron distribution, described by Eq. (2) with loss cone, is (Wentzel 1976)

$$\frac{\Gamma}{\Omega} \approx \frac{\pi}{2}\frac{\delta}{\gamma}\frac{n_1}{n}\left(A - \frac{\omega}{kc}\right), \tag{4}$$

where A is the anisotropy measure that can by represented for the loss-cone anisotropy as $A = (\sigma - 1)^{-1}$, $\sin^2\theta^* = \sigma^{-1}$. For $\delta = 5$ with $\omega/kc \ll A$ and $\gamma = 3$, we have

$$\Gamma/\Omega \approx 2.6 A n_1/n. \tag{5}$$

From the phase velocity plot (Fig. 6) we conclude that for the 1999 August 28 flare whistlers with the relative phase velocity $\omega/kc \approx 0.03$ have the frequency $x \geq 0.95$. These high-frequency whistlers undergo, however, strong cyclotron damping on electrons of thermal background plasma. Indeed the damping rate (Alpert 1982) is

$$\nu/\Omega = (\pi/2)^{1/2}[(1-x)(c/V_\mathrm{T})/N] \times \exp\{-[(1-x)^2(c/V_\mathrm{T})^2/2(Nx)^2]\}, \tag{6}$$

where $V_\mathrm{T} = (\kappa T/m)^{1/2}$ is the electron thermal velocity of the loop's background plasma. For example, for the frequency $x = 0.95$ and plasma temperature $T = 2 \times 10^6$ K, we obtain $\nu/\Omega \approx 10^{-1}$. Comparing this value with the growth rate (Eq. (5)), we find an instability threshold of $n_1/n > 10^{-1}/2.6A$. Because from radio observations we obtained $n_1/n \approx 4.3 \times 10^{-7}$ and the anisotropy measure $A \leq 1$, we see that there is no instability for high-frequency whistlers. Moreover the resonance condition (Eq. (3)) suggests that high-frequency whistlers $x \geq 0.9$ interact with low-energy (≈10 keV) electrons. These electrons, however, do not contribute to the gyrosynchrotron emission at 17 GHz. Hence we have to consider low-frequency whistlers.

The strong diffusion regime means that, due to pitch-angle scattering, only slight anisotropy is presented in an electron cloud (Trakhtengerts 1984; Bespalov & Efremova 1993). Indeed, just immediately after injection for the time of about $10/\Gamma \approx 3.8 n/A_0 \Omega n_1 \approx 3 \times 10^{-3}$ s, which is much less then the free travel time of fast electrons $t_0 = L/c \approx 0.23$ s, the quasi-linear pitch-angle diffusion of particles on small-scale turbulence makes the electron distribution nearly isotropic. Here we suggest that the initial anisotropy measure $A_0 = (\sigma - 1)^{-1} \approx 1.0$, $n/n_1 \approx 2.3 \times 10^6$, and $\Omega \approx 2.6 \times 10^9$ s^{-1}. It is known that the pitch-angle diffusion rate is much larger than the momentum diffusion rate $(\Delta\theta/\theta)/(\Delta p/p) = (k_\parallel p_\parallel/m\omega - 1) \gg 1$ because $k_\parallel p_\parallel/m \approx \Omega \gg \omega$ (Melrose 1980). In this case we have the very small anisotropy of fast electrons propagating along a loop. For the faint anisotropy $A \ll 1$, the frequency of excited whistlers of $\omega < A\Omega \ll \Omega$. Taking, for example, the waves with a phase velocity $\omega/kc \approx 0.03$ (refractive index $N \approx 30$) from Eqs. (1) and (3) for 1 MeV electrons ($\gamma = 3$) we have $x \approx (\gamma N)^{-1} \approx 10^{-2}$ (e.g. $\omega \approx 20\Omega_i$) and $y \approx Nx^{1/2} \approx 3$. For 500 keV and 2 MeV electrons, we obtain correspondingly $x \approx 1.7 \times 10^{-2}$ ($\omega \approx 30\Omega_i$), $y \approx 3.9$, and $x \approx 6.7 \times 10^{-3}$ ($\omega \approx 12\Omega_i$), $y \approx 2.4$.

In fact we do not know the actual distribution function of high-energy electrons. In order to interpret the NoRH data, we suppose that gyrosynchrotron emission is generated by electrons with a power-law spectrum. It is not excluded that electron distribution was far from power-law. Moreover, the electron fluxes can have quite a large dispersion $\Delta E \approx E_\mathrm{res} \approx 1$ MeV.

The above-considered approximation of a homogeneous plasma is a fairly rough idealization of real magnetic loops. Because a real loop is inhomogeneous throughout a loop radius and a loop length, it means that a whistler-wave spectrum can be quite broad. In our example for electrons with energies (0.5–2.0) MeV, the wave-particle interaction will be in the frequency band $\omega \approx$ (12–30) Ω_i. The wavelength band of whistlers interacting at a cyclotron resonance with (0.5–2.0) MeV electrons is $\lambda = 2\pi/k \approx$ 1.4–3.6 m.

Following from Eq. (6) for $\omega \ll \Omega$ gyroabsorption of whistlers on the electrons of the thermal background plasma is negligible and a minimal value of the whistler instability threshold is determined by the Coulomb-collision damping with the decrement

$$\nu_\mathrm{c} = x\nu_\mathrm{ei}, \quad \nu_\mathrm{ei} \approx 60 n T^{-3/2}. \tag{7}$$

When comparing Eqs. (5) and (7), we obtain for $A \approx 0.1$, $n \approx 7 \times 10^9$ cm^{-3}, and $T \approx 2 \times 10^6$ K an instability threshold for the density of energetic particles $(n_1/n)_\mathrm{min} > \nu_{ei} x/2.6A\Omega \approx 2 \times 10^{-9}$, which is far below the relative number density of ≥0.5 MeV electrons, $n_1/n \approx 4.3 \times 10^{-7}$.

Besides cyclotron and the Coulomb-collision damping of the whistler waves, there is Landau damping, which can break off the strong diffusion regime in a loop (Stepanov & Tsap 2002). Indeed, whistlers propagating parallel to the magnetic field do not suffer Landau damping since the longitudinal component of the electric field of waves equals zero. However, during propagation in the curved magnetic field of the loop, whistlers generate a small electric field parallel to $\boldsymbol{B}$, and therefore Landau damping can occur with the damping rate (Akhiezer et al. 1975):

$$\nu_L/\Omega \approx (\sqrt{\pi}/4)\phi(z) x^2 \sin^2\psi. \tag{8}$$

Here $z = \omega/\sqrt{2}(kV_T)$, ψ is the angle between the wave vector and the magnetic field. In our case $z = 1.3$, thus the values of the function $\phi(z) \approx 0.3$ (Akhiezer et al. 1975). Comparing Eqs. (5) and (8) with $A \approx 0.1$, $x \approx 10^{-2}$, we obtain the instability threshold against the Landau damping

$$n_1/n \approx 5 \times 10^{-5} \sin^2\psi. \tag{9}$$

Putting the earlier estimate of $n_1/n \approx 4.3 \times 10^{-7}$ into Eq. (9), we concluded that low-frequency whistlers do not undergo Landau damping within the domain $\psi \approx 5.3$ degrees. Because of the loop length of about 7×10^9 cm, we can find the minimum value of the loop thickness needed to avoid Landau damping of whistler

waves from simple geometrical considerations: $\approx 3\times10^8$ cm. The extended source in the 1999 August 28 flare with a thickness of about 10^9 cm does not fit this condition well. Thus the low-frequency whistlers undergo strong Landau damping outside the narrow domain $\psi < 5$ degrees; i.e. they can grow in amplitude while propagating only almost parallel to the magnetic field.

What is the way out? There are indications of a fine (sub-arcsecond) structure of coronal loops through the loop radius. In order to explain the near-isothermal appearance of a loop from TRACE observations, Reale & Peres (2000) proposed a multi-thread model. The multi-thread concept was applied by Aschwanden et al. (2000) to studying the nonuniform heating of coronal loops based on TRACE data, and they suggested the loop filaments with a typical cross-sectional dimension of about 0.1 arcsec. The mechanism of loop plasma heating proposed by Zaitsev & Shibasaki (2005) also requires filamentation of a loop with the cross-sectional scale $\sim10^6$ cm. Filaments with the temperature and density stratification are in fact the ducts (wave guides) for whistler waves. The whistlers propagate in ducts along the magnetic field without substantial Landau damping, and the lower instability threshold for parallel propagation is actually determined by Coulomb collisions $n_1/n > 2\times10^{-9}$. Before that we found that low-frequency whistlers with phase velocity $c/30$ fit both resonance condition and dispersion equation better if $y \approx 3$. It means that plasma density in a loop should be about 2×10^{10} cm^{-3}, which is three times more than the pre-flare density. Loop filamentation can supply these conditions.

It should also be noted that analysis of quasi-periodic modulation of microwave emission (Stepanov et al. 2004) in the 1999 August 28 flare gives the following parameters averaged on an entire extended loop: plasma density can be as high as $n \approx 2\times10^{10}$ cm^{-3}, the temperature $T \approx 2\times10^7$ K, and the magnetic field $B = 100$–200 G. Hence there are satisfactory conditions in coronal magnetic loops for generating low-frequency whistler turbulence and a turbulent "wall" formation.

4.2. "Wall" due to Langmuir wave turbulence?

Here we supposed that gyrosynchrotron emission at 17 and 34 GHz is generated by electrons with a power-law spectrum (index $\delta = 5$). It was also mentioned that whistlers have quite a low instability threshold under coronal conditions. Nevertheless, if high-energy electrons have a loss-cone type anisotropy of (except for electrons with a power-law distribution), or else bump-in-tail type, the excitation of longitudinal waves is possible. Such waves can be the plasma waves near the electron plasma frequency (due to beam instability) or upper hybrid waves (due to loss-cone instability). Bespalov & Efremova (1993) studied a self-consistent case where an anisotropic cloud of high-energy electrons generate plasma waves in dense plasma, $\omega_p^2 \gg \Omega^2$. The typical feature of the self-consistent expansion of energetic electrons is the formation of a turbulent "wall" on its front. Due to strong diffusion, the initial anisotropy therefore reduces rapidly and excited plasma waves have a much lower phase velocity than a particle's average velocity V (Bespalov & Trakhtengerts 1974):

$$V_{\rm ph} = V(4\nu n/\omega_p n_1)^{1/3}. \quad (10)$$

For $V = c$, $\nu = \nu_{ei} \approx 1.5\times10^2$ s^{-1}, $\omega_p \approx 5\times10^9$ s^{-1}, from Eq. (10), we obtain $V_{\rm ph}/c \approx 0.03$ if $n/n_1 \approx 3\times10^2$. We see that this mechanism explains the observed velocities if the high-energy electron cloud is quite dense. Because observations give $n/n_1 \approx 10^6$ we concluded that the "turbulent wall" in the 1999 August 28 event can not be formed by Langmuir wave turbulence.

5. Discussion

We have shown that, due to the excitation of low-frequency whistlers by the group of high-energy electrons injected into a coronal loop, these electrons can propagate along the loop axis with the whistler phase velocity, which is about 30 times lower than the particle velocity. The total energy of the injected electron cloud is about $n_1(\pi r^2 L)E \approx 3\times10^{25}$ erg. Here we used parameters deduced from both observations and our model: $n_1 \approx 3\times10^3$ cm^{-3}, $r \approx 5\times10^8$ cm, $L \approx 7\times10^9$ cm, average energy of electrons $E \approx 1$ MeV $\approx 1.6\times10^{-6}$ erg. We see that the population of electrons injecting into the loop and generating emission at 17 GHz contains a small part of the thermal plasma energy in the loop, $n_1E/n\kappa T \approx 2\times10^{-3}$. To check our model let us remember that, in accordance with the strong diffusion regime, the lifetime of trapping electrons in a loop $t_{\rm strong} \approx \beta^* t_0$ must exceed the particle lifetime in a weak diffusion regime $t_{\rm weak} \approx \sigma t_0$ (Trakhtengerts 1984). Here $\beta^* = 8\pi nE/B^2$. With $n \approx 10^{10}$ cm^{-3}, $E \approx 1$ MeV, and a medium value of the magnetic field along the extended loop $B \approx 150$ G, we obtain $\beta^* \approx 20 \gg \sigma$. We see that our suggestion about strong diffusion is satisfied. The reasons for a higher plasma density ($y \approx 3$) in the impulsive phase can be a denser plasma in a loop–loop interaction site and loop filamentation.

The 1999 August 28 flare looks similar to the double-loop event studied by Hanaoka (1999). In accordance with our model, the loop–loop interaction is an injector of high-energetic electrons into the large-flare loop. A first injection of relativistic electrons at 00:56:10 UT responsible for microwave emission was powerful enough to form a turbulent "wall", $I \gg I^*$.

As mentioned in Sect. 1, two cases of turbulent propagation of high-energy particles are possible (Bespalov & Efremova 1993). The first case considers propagation of charged particle through the pre-existing plasma turbulence. The second self-consistent case suggests that particle flux generates the small-scale waves itself and forms a turbulent "wall" on its front. The important peculiarity of the last case is that turbulent propagation velocity increases in time for the self-consistent expansion of a cloud. There are some indications of increase a velocity during the events "A" (Fig. 3). Also, it is difficult to imagine the origin of the pre-excited low-frequency whistler turbulence in the magnetic loop structure before a flare. It would be reasonable to conclude that low-frequency whistlers are generated effectively by the high-energy electron fluxes themselves.

Note that the high speed $\approx 10^5$ cm/s propagation of microwave source started at 00:56:19.5 UT (line "B" in Fig. 3) and indicates the different physical conditions in the large flaring loop compared with the case "A". These conditions were unfavorable for the whistler excitation. Indeed, the situation in the course of the first electron injection privileged the generation of the whistler waves because the loss cone of a loop is almost empty in the beginning of the flare. In this case the instability criterion for the anisotropy of high-energy electrons $A > \omega/kc \approx 0.03$ (see Eq. (4)) was easily satisfied. The second injection started when the loss cone was filled in by precipitating electrons, and therefore the inequality $A > \omega/kc$ was not satisfied, so the turbulent "wall" in case "B" was not formed.

6. Conclusions

There are two main effects of strong diffusion that is due to wave-particle interaction: (i) izotropization of the particle distribution; (ii) particle propagation with the velocity of about phase velocity of waves generated by the particles themselves.

The flare burst of 1999 August 28 was well-observed with high spatial resolution by the Nobeyama Radioheliograph in the microwave range, as well as by GOES (soft X-rays), BATSE (hard X-rays), and in optic wavelengths (SOHO/MDI). This burst gives us a good example of the turbulent propagation of high-energy electrons in the solar coronal plasma. The physical reasons for this "turbulent expansion" are as follows:

1. Electrons in a loop must be relativistic or nearly relativistic to produce gyrosynchrotron emission at 17 and 34 GHz.
2. The same population of electrons generates the low-frequency whistlers.
3. Requirements for strong turbulent diffusion are satisfied: the source power of injecting relativistic electrons is high enough, $I \gg I^* = 2 \times 10^{11}$ cm^{-2}s^{-1}, and $\beta^* \gg \sigma$.
4. To avoid Landau damping of the whistlers, the loop has to consist of filaments (ducts).

We conclude that the solar event of 1999 August 28 presents a good illustration of the collective effects of interaction of high-energy particles with small-scale turbulence in astrophysical plasma.

Acknowledgements. A.V.S. and V.F.M. acknowledge an invitation to the Nobeyama Radio Observatory of the National Astronomical Observatory of Japan. We also thank P. A. Bespalov and V. Yu. Trakhtengerts for a fruitful discussion. The work was partly supported by RFBR grants NN. 06-02-16859, 04-02-39029, 04-02-16753.

References

Alexander, D. 1990, A&A, 235, 431
Alpert, Ya.L. 1982, The Near-Earth and Interplanetary Plasma (Cambridge Univ. Press), 1
Aschwanden, M. J. 2002, Space Sci. Rev., 101(1-2)
Aschwanden, M. J., Nightingale, R. W., & Alexander, D. 2000, ApJ, 541, 1059
Akhiezer, A. I., Akhiezer, I. A., Polovin, R. V., Sitenko, A. G., & Stepanov, K. N. 1975, Plasma Electrodynamics, Linear Theory (Pergamon Press), 1
Batchelor, D. A., Crannel, C. J., Wiel, H. J., & Magun, A. 1985, ApJ, 295, 258
Bastian, T. S. 1999, Solar Physics with Radio Observation, Proc. Nobeyama Symp., NRO Rep. 479, 211
Bastian, T. S., Nitta, N., Kiplinger, A. L., & Dulk, G. A. 1994, Proc. Kofu Symp., NRO Rep. No. 360, 199
Bespalov, P. A., & Trakhtengerts, V.Yu. 1974, ZhETF, 67, 969 (in Russian)
Bespalov, P. A., & Efremova V. G. 1993, Planet. Space Sci., 41, 785
Bespalov, P. A., Zaitsev, V. V., & Stepanov, A. V. 1987, Sol. Phys., 114, 127
Bespalov, P. A., Zaitsev, V. V., & Stepanov, A. V. 1991, ApJ, 374, 369
Brambilla, M. 1998, Kinetic Theory of Plasma Waves: Homogenous Plasma (Oxford: Clarendon Press)
Brown, J. C., Melrose, D. B., & Spicer, D. S. 1979, ApJ, 228, 592
Budker, G. I., Mirnov, V. I., & Rytov, D. D. 1971, Pisma ZhETF, 14, 320 (in Russian)
Dulk, G. A. 1985, ARA&A, 23, 169
Fleishman, G. D., & Melnikov, V. F. 2003, ApJ, 587, 823
Fletcher, L. 1997, A&A, 326, 1259
Hanaoka, Y. 1999, PASJ, 51, 483
Hulot, E., Vilmer, N., & Trottet, G. 1989, A&A, 213, 383
Lee, J. W., & Gary, D. F. 1994, Sol. Phys., 153, 347
Lee, J., Gary, D. E., & Shibasaki, K. 2000, ApJ, 531, 1109
MacKinnon, A. L. 1991, A&A, 242, 256
Melnikov, V. F., & Magun, A. 1998, Sol. Phys., 178, 153
Melnikov, V. F., Shibasaki, K., & Reznikova, V. E. 2002, ApJ, 580, L185
Melnikov, V. F. 2006, in Solar Physics with the Nobeyama Radioheliograph, Proc. Nobeyama Symposium (Kiosato, 26–29 October 2004), ed. K., Shibasaki, NSRO Report No. 1, 9–20
Melrose, D. B. 1980, Plasma Astrophysics (Gordon & Breach), 2
Melrose, D. B., & Brown, J. C. 1976, MNRAS, 176, 15
Ramaty, R. 1969, ApJ, 158, 753
Reale, F., & Peres, G. 2000, ApJ, 528, L45
Sakai, J. I., & de Jager, C. 1996, Space Sci. Rev., 77, 1
Shibasaki, K. 2001, ApJ, 557, 32
Smith, D. F., & Lillienquist, C. C. 1979, ApJ, 232, 582
Stepanov, A. V., & Tsap Yu.T. 2002, Sol. Phys., 211, 135
Stepanov, A. V., Kopylova, Yu. G., Tsap, Yu. T., Shibasaki, K., et al. 2004, Astronomy Lett. 30, 480
Trakhtengerts, V. Yu. 1984, Relaxation of Plasma with Anisotropic Velocity Distribution, ed. A. A., Galeev, R. N., Sudan, Basic Plasma Physics II (North-Holland Physics Publishing)
Wentzel, D. G. 1976, ApJ, 208, 595
White, S. M., Janatdhan, P., & Kundu, M. R. 2000, ApJ, 533, L167
Yokoyama, T., & Shibata, K. 1995, Nature, 375, 42
Yokoyama, T., Nakajima, H., Shibasaki, K., Melnikov, V. F., & Stepanov, A. V. 2002, ApJ, 576, L87
Zaitsev, V. V., & Shibasaki, K. 2005, Astron. Rep., 49, 1009